

ENERGY DISTRIBUTION FUNCTIONS OF ARGON IONS IN LOW CURRENT, DIFFUSE DISCHARGES AT HIGH  $E/N$ S. B. Vrhovac<sup>†</sup>, B. M. Jelenkovic<sup>†</sup>, J. K. Olthoff\* and R. J. Van Brunt\*<sup>†</sup>Institute of Physics, P. O. Box 57, 11001 Belgrade, Yugoslavia

\*National Institute of Standards and Technology, Gaithersburg, MD 20899 USA

## INTRODUCTION

Surface modification using plasma assisted etching and deposition has been largely based on the interactions of neutrals and ions with the substrate. It is of interest therefore to know more about ion impact energy distribution functions, the composition of the ion flux at the substrate, and the directionality of ions in discharges used to process different materials. There is a need to better understand the behavior of ions in the cathode sheath of argon glow discharges, because argon is often used in plasma sputtering and as a reference gas in plasma processing experiments. There are several investigations of ion kinetic energies and angular distributions in both dc [1] and rf [2] discharges for pressures ranging from 0.13 Pa. to 0.13 kPa. Additionally, the ion energy distribution functions have been calculated using either Monte Carlo models [2] or by assuming that ions are in hydrodynamic equilibrium at a particular local electric field-to-gas density ratio ( $E/N$ ) [1,3].

Previous investigations [4] have been limited to determinations of the energy distribution function (EDF) of  $\text{Ar}^+$  ions drifting in neutral argon gas for  $E/N$  only up to 300 Td ( $1 \text{ Td} = 10^{-21} \text{ Vm}^2$ ). In this work we present results from measurements of the EDF for  $\text{Ar}^+$  and  $\text{Ar}^{2+}$  in dc, low-current, diffuse argon discharges with  $E/N$  ratios ranging from 640 Td to 41 kTd. Our measurements of EDF were done using both a retarding potential analyzer (RPA), and a cylindrical mirror analyzer (CMA) [5]. These measurements allow a test of predicted "steady-state" energy distribution functions for  $\text{Ar}^+$  [3].

## EXPERIMENT

Two drift tubes were used to study the kinetic-energy distributions of ions sampled from low-current, low-pressure argon discharges. Each consisted of stainless-steel parallel-plane electrodes placed in a quartz cylinder in order to prevent long path breakdown. One drift tube utilized a 4-grid RPA for ion energy analysis, and has been described elsewhere [6]. For this apparatus, the electrode diameter was 40 mm with an electrode spacing of 20 mm. The ions from the discharge entered the RPA through a pattern of seven 0.1-mm holes in the cathode.

The other drift tube was appended to a cylindrical mirror energy analyzer with a quadrupole mass spectrometer (CMA-MS) which allowed the identification of the ion mass. A schematic diagram of this apparatus is shown in Fig. 1. The drift tube consisted of 20-mm parallel plane stainless-steel electrodes with an interelectrode spacing of 12 mm. The discharge was operated at pressures ranging from 23 Pa to 124 Pa with a discharge current of 8  $\mu\text{A}$ . Ions were sampled from the discharge through an 0.28-mm hole and then entered the CMA-MS through an 0.2-mm hole in the CMA-MS sampling

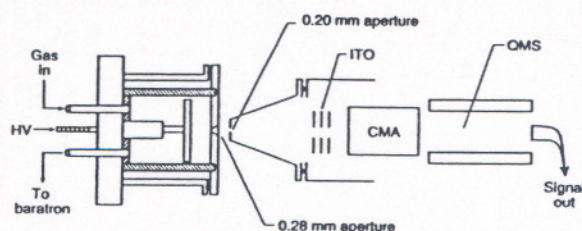


Figure 1. Schematic diagram of the cylindrical mirror ion energy analyzer with quadrupole mass spectrometer (QMS) attached to a parallel-plate drift tube. ITO are the ion-transfer lenses.

cone. The double aperture arrangement was utilized to keep the pressure in the mass spectrometer portion of the vacuum system below  $10^{-5} \text{ Pa}$  ( $\sim 10^{-7} \text{ Torr}$ ). Pressures in the intermediate region between the two apertures was near  $10^{-3} \text{ Pa}$  ( $\sim 10^{-5} \text{ Torr}$ ). The CMA was operated in a mode such that an energy resolution of 2 eV was maintained over the entire energy range scanned. Corrections were made to the ion kinetic-energy scale to compensate for surface charging in the vicinity of the apertures [7].

## RESULTS AND DISCUSSIONS

The measured kinetic-energy distribution functions of  $\text{Ar}^+$  and  $\text{Ar}^{2+}$  at different  $E/N$  are shown in Figs. 2 and 3, respectively, as measured by the CMA-MS. No  $\text{Ar}_2^+$  ions were detected from the discharge, presumably because  $E/N$  values were too large in the discharge to promote the required three-body, low-energy interactions. For  $\text{Ar}^+$ , the EDF exhibit an exponential decay as the ion energy increases for  $E/N$  below 5 kTd. However, for higher  $E/N$  there is a deficiency of ions with energies above approximately 40 eV. This deficiency is also observed for  $\text{Ar}^{2+}$  as seen in Fig. 3. The deficiency of ions above 40 eV suggests the possibility that higher energy ions may be lost from the solid angle of the detector as a result of inelastic and/or elastic collisions. Collisional effects of  $\text{Ar}^+$  ions leading to scattering of ions outside the collection angle of the experiment will be further investigated and discussed at the conference.

Kinetic-energy distribution functions from argon discharges at higher  $E/N$  values were measured using the drift tube with the RPA. These are presented in Fig. 4. While no mass analysis is available on this instrument, the ion signal is almost entirely  $\text{Ar}^+$  at high  $E/N$  so these data may be compared directly with those in Fig. 2. Note that no deficiency of ions with higher energies are observed for this instrument, although the high energy tails of the distributions exhibit deviations from the Maxwellian form given below.

The mobility of  $\text{Ar}^+$  ions in their parent gas is mainly determined by charge-exchange collisions. The distribution function for ions drifting through a uniform electric field are predicted to be Maxwellian



from solutions of the Boltzmann equation [3], i.e.,

$$f(\epsilon) = (kT^+) \exp(-\epsilon/kT^+) \quad (1)$$

where  $kT^+ = eE/(NQ_{CT})$  is an ion "temperature", and  $Q_{CT}$  is the cross section for resonant charge transfer in  $\text{Ar}^+ + \text{Ar}$  collisions.

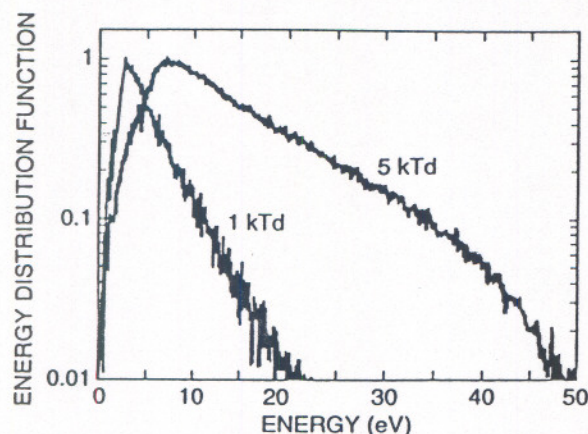


Figure 2. Energy distribution function,  $f(\epsilon)$ , of  $\text{Ar}^+$  at 1000 and 5000 Td as measured using the CMA-MS apparatus.

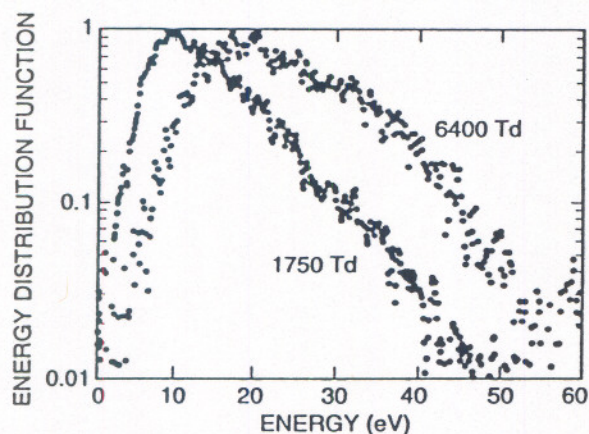


Figure 3. Energy distribution function,  $f(\epsilon)$ , of  $\text{Ar}^{++}$  at 1750 Td and 6400 Td as measured using the CMA-MS apparatus.

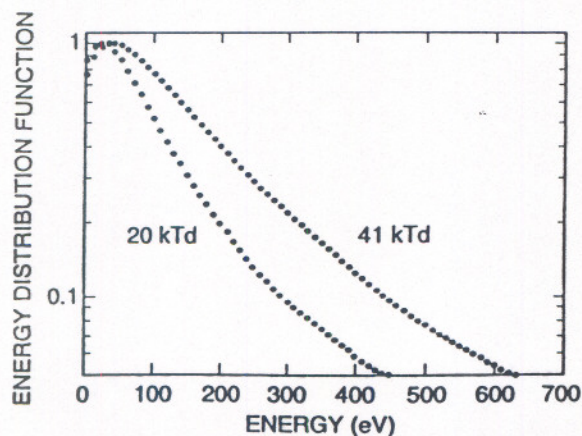


Figure 4. Energy distribution function,  $f(\epsilon)$ , of  $\text{Ar}^+$  at 20 kTd and 41 kTd as measured using the RPA apparatus.

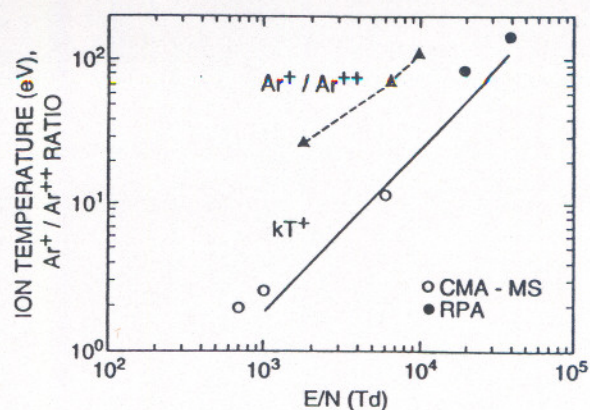


Figure 5. Measured (circles) and calculated (solid line) ion temperatures,  $kT^+$ , and ratios of  $\text{Ar}^+/\text{Ar}^{++}$  fluxes (triangles) versus  $E/N$ .

The ion velocity in the direction of the field,  $v_z$ , is much greater than the thermal component perpendicular to the electric field so that  $\epsilon = mv_z^2/2$ , where  $m$  is the ion mass.

Figure 5 shows the ion temperatures for  $\text{Ar}^+$  versus  $E/N$  as determined by the linear portion of the data in Figs. 2 and 4, and as calculated by the expression in Eq. (1). The data points for  $E/N$  values below 10 kTd were derived from measurements made with the CMA, while data points at higher  $E/N$  were obtained with the RPA. There is good agreement between the different experimental techniques, and between experimental and calculated values for the apparent ion "temperature". The data for the charge-transfer cross sections of  $\text{Ar}^+ + \text{Ar}$  used in Eq. (1) were taken from Ref. [8].

Shown with solid triangles, and connected with a dashed line on Fig. 5, is the ratio of singly and doubly charged ion flux versus  $E/N$ . The  $\text{Ar}^+$  ions dominate the ion flux for the  $E/N$  values studied here. For  $E/N$  values greater than 10 kTd, the  $\text{Ar}^+/\text{Ar}^{++}$  ratio exceeds 100. The increase of  $\text{Ar}^+$  flux in comparison with  $\text{Ar}^{++}$  for increasing  $E/N$  conditions is expected because of the lower threshold for single ionization by electron impact. The rates for processes involving the direct ionization of neutrals by electrons can change significantly with changes in the electron-energy distribution function associated with changing  $E/N$ .

There is a large decrease in the total ion current arriving at the CMA-MS sampling cone as the  $E/N$  value in the discharge decreases below 1500 Td. We were unable to detect an  $\text{Ar}^{++}$  signal with the CMA-MS for  $E/N$  values below 1000 Td, and the  $\text{Ar}^+$  signal disappeared for values below about 600 Td. This determines the lower  $E/N$  limit of our measurements. Similar detection limits have been observed for the RPA drift tube when the same plate separation (12 mm) is used. Since the measurements of EDF at low  $E/N$  suggest that the dominant collision process is charge transfer, the reason for low signal/noise ratios at low  $E/N$  and higher gas densities may be the short mean free path of ions with respect to the thickness of the field-free region between the cathode and the CMA entrance aperture or between the cathode and the RPA grids, where the gas pressure is still relatively high.

#### ACKNOWLEDGEMENTS

This work was supported, in part, by the YU-USA Joint program for scientific collaboration under project JF 924. The National Insti-



tute of Standards and Technology contribution was performed in the Electricity Division, Electronics and Electrical Engineering Laboratory, Technology Administration, U. S. Department of Commerce. The authors wish to thank A. V. Phelps for helpful discussions.

#### REFERENCES

1. Davis, W. D., and Vanderslice, T. A., 1963, *Phys. Rev.* **131**, pp. 219.
2. Lin, J., Huppert, G. L., and Sawin, H. H., 1990, *J. Appl. Phys.* **68**, pp. 3916.
3. Lawler, J. E. 1985, *Phys. Rev. A* **32**, pp. 2977; Wannier, G. H., 1966, *Statistical Physics* (Wiley, New York), pp. 462.
4. Ong, P. P. and Hogan, M. J., 1985; *J. Phys. B*, **18**, 1987.
5. Sor-el, H. Z., 1967, *Rev. Sci. Instrum.*, **38**, pp. 1210.
6. Vrhovac, S. B., Radovanov, S. B., Petrovic, Z. Lj., and Jenkovic, B. M., 1992, *J. Phys. D*, **25**, pp. 217.
7. Makabe, T., and Shinada, H., 1985, *J. Phys. D*, **18**, 2385.
8. Cramer, W. H., 1959, *J. Chem. Phys.*, **30**, pp. 641.